THE JOURNAL OF PHYSICAL CHEMISTRY B

Article

pubs.acs.org/JPCB

Stable Salt−Water Cluster Structures Reflect the Delicate Competition between Ion−Water and Water−Water Interactions

Cheng-Wen Liu,[†] Feng Wang,[∥] Lijiang Yang,[†] Xin-Zheng Li,[‡] Wei-Jun Zheng,*[,§] and Yi Qin Gao*[,†]

[†]Institute of Theoretical and Computational Chemistry, College of Chemistry and Molecular Engineering, Beijing National Laboratory for Molecular Sciences, Peking University, Beijing 100871, China

[‡]School of Physics, Peking University, Beijing 100871, China

[§]Beijing National Laboratory for Molecular Sciences, State Key Laboratory of Molecular Reaction Dynamics, Institute of Chemistry, Chinese Academy of Sciences, Beijing 100190, China

[∥]Department of Chemistry and Biochemistry, University of Arkansas, Fayetteville, Arkansas 72701, United States

Supporting Information

ABSTRACT: How salts affect water structure is an important topic in many research fields. Salt−water clusters can be used as model systems to extract interaction information that is difficult to obtain directly from bulk solutions. In the present study, integrated tempering sampling[1,2] molecular dynamics (MD) are combined with quantum mechanics (QM) calculations to overcome the sampling problem in cluster structure searches. We used $LiI(H_2O)_n$ and $CsI(H_2O)_n$ as representatives to investigate the microsolvation of ion pairs. It was found that Li^+−I^- and Cs^+−I^- ion pairs interact with water molecules in very different ways, and the corresponding salt−water clusters have distinctly different structures. LiI strongly affects water−water interactions, and the $LiI(H_2O)_n$ ($n \geq 5$) clusters build around a $Li^+(H_2O)_4$ motif. CsI only slightly perturbs the water cluster structure, and $CsI(H_2O)_n$ favors the clathrate-like structure when n = 18 or 20. Consistent with the law of "matching water affinities", Li^+ and I^- are more easily separated by solvent molecules than the Cs^+−I^- ion pair.

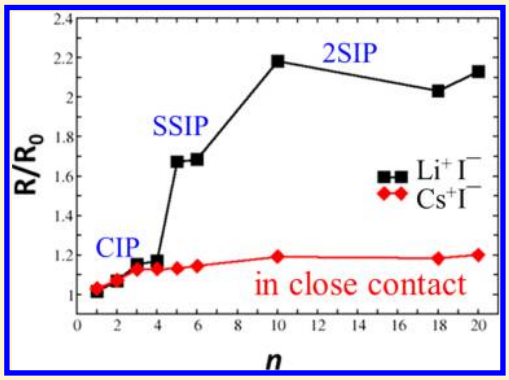

INTRODUCTION

Solvation of ion pairs in water is a topic that attracts much research interest because of its importance in fields such as biochemistry,[3] marine chemistry,[4] and atmospheric chemistry.[5−7] Although the solvation of ion pairs in bulk water likely involves a large number of water molecules and depends on the bulk properties of water, it is instructive to investigate their microsolvation starting from small salt−water clusters, which can be used to characterize in more detail the different ion−water interactions.

It has long been known that ions have specific effects on water properties. For example, ions influence the liquid−air surface tension and the solubility of proteins.[8−11] In the Hofmeister series, cations and anions are ranked according to their ability to "salt in" or "salt out" proteins from aqueous solutions. For cations, a rather common order is[12]

$$Cs^+ > Rb^+ > NH_4^+ > K^+ > Na^+ > Li^+ > Ca^{2+} > Mg^{2+} > Zn^{2+}$$

The ions on the left side tend to promote the displacement of water from the solvation layer of proteins and thus stabilize protein structures. On the other hand, the ions on the right side tend to promote the solvation of proteins and thus denature them.[13]

Among inorganic salts, due to their chemical and biological significance and relative simplicity, the alkali halide salts have attracted the most attention. Although numerous experimental[14−21] and theoretical[22−42] studies have been conducted on both bulk solution and salt−water clusters, many questions on ion solvation remain unanswered. To understand the Hofmeister series, it is instructive to interrogate how different ions (ion pairs) interact differently with water using salt−water clusters as simplified models. In the present study, we chose two alkali cations, Cs^+ and Li^+, at rather different positions in the Hofmeister series to study their ion-pairing behavior with I^- in water clusters. We also note that the solubility of LiI in water at room temperature is twice that of CsI, which means the two ion pairs probably have very different hydrations. These differences make CsI−water and LiI−water clusters good model systems to understand the Hofmeister series. In a recent study,[43] we used photoelectron spectroscopy and density functional theory (DFT) to study $LiI(H_2O)_n$ and $CsI(H_2O)_n$ (where n = 0−6) clusters in their anionic and neutral states. We found that the structures of $LiI(H_2O)_n$ and $CsI(H_2O)_n$ clusters are indeed very different. One purpose of the current study is to

Received: August 22, 2013
Revised: December 23, 2013
Published: January 3, 2014

examine how the differences between the two types of clusters evolve as the sizes of the clusters increase further. The larger clusters presumably represent the bulk solutions more closely.

One outstanding difficulty in computational study of large water and salt−water clusters lies in the large configuration space of the clusters, which contains many potential energy minima. It is computationally challenging to locate all the stable isomers. In the present study, to address this challenge, we used integrated tempering sampling (ITS)[1,2] molecular dynamics to generate ensembles of structures with low configuration energies. ITS allows efficient sampling of structures over a very controlled but broad energy range and thus permits fast identification of low-energy structures and transition states. The resulting structures are then optimized using both classical force field and DFT functionals.

We first tested the performance of ITS for this specific application by searching for low-energy structures of pure-water clusters $(H_2O)_{12}$ and $(H_2O)_{20}$. With ITS, structural transitions over potential energy barriers are largely facilitated; in addition, ITS frequently visits structures with lower energies, thus enabling the identification of many low-energy structures. For water clusters, we perform energy minimizations with the SPC/E force field starting from low-energy structures identified by ITS. The SPC/E structures were then optimized with the BLYP-M2 method[44] custom-made to give a coupled cluster quality potential energy surface for water clusters. In addition to previously reported local minima,[45−53] a new low-energy structure is found for the $(H_2O)_{12}$ cluster and another one for $(H_2O)_{20}$. This success in obtaining the low-energy structures of water clusters validates the usage of ITS for conformational search.

A similar procedure was followed for salt−water clusters, $LiI(H_2O)_n$ and $CsI(H_2O)_n$ (n = 10, 18, and 20). The results showed that the structures of clusters consisting of the two salts are distinctly different. The $CsI(H_2O)_{10}$ shares similar low-energy structures with $(H_2O)_{12}$, with two water molecules replaced by Cs^+ and I^-. In contrast, Li^+ and I^- cause significant perturbation to the structure of the $(H_2O)_{12}$ cluster, with Li^+ being strongly hydrated. Similarly, we found that Li^+ is strongly hydrated in both $LiI(H_2O)_{18}$ and $LiI(H_2O)_{20}$ clusters, whereas $CsI(H_2O)_{18}$ and $CsI(H_2O)_{20}$ clusters tend to form clathrate-like structures, with Cs^+ residing in the center of a cage formed by water molecules and I^- ion. The lowest energy structures of $CsI(H_2O)_{18}$ resemble well the clathrate-like structure of $(H_2O)_{20}$. These results suggest that the balance between the ion−water and water−water interactions plays an important role in determining the overall structure of salt−water clusters. In the meantime, the ITS MD simulations also provide detailed information on the temperature dependence of the structural properties of the two types of water−salt clusters.

The paper is organized as follows: In section 2, we describe the computation details. The results are presented and discussed in section 3, and the conclusions are drawn in the last section.

■ COMPUTATIONAL DETAILS

The SANDER module of the AMBER9.0 software package[54] was used for ITS and MD simulations. The three-point-charge SPC/E[55] model was used for water molecules, and the popular ion parameters, ions08,[56] were used for Li^+, Cs^+, and I^- ions. The ion−water cross-terms were calculated with the Lorentz−Berthelot combination rules. All simulations were integrated with a time step of 0.5 fs. For MD simulations performed to compare with ITS, the temperatures were maintained at 200 K for $(H_2O)_{12}$ and $MI(H_2O)_{10}$ (M = Li, Cs) and 170 K for $(H_2O)_{20}$ and $MI(H_2O)_n$ (M = Li, Cs; n = 18 and 20) using Langevin dynamics[57] with a collision frequency of 1 ps^{-1}. All simulations were performed in a vacuum without a periodic boundary condition. To ensure all the pairwise interactions between all the molecules in the cluster are fully accounted for, non-bonding interaction cutoffs were set to be 30 Å for $(H_2O)_{12}$ and $MI(H_2O)_{10}$ (M = Li and Cs) and 50 Å for $(H_2O)_{20}$ and $MI(H_2O)_n$ (M = Li and Cs; n = 18 and 20). All the structures in this paper were visualized and rendered using the VMD program.[58]

The details of the ITS method have been described previously.[1,2] Briefly, in the ITS simulation, a modified potential energy is obtained from a summation of Boltzmann factors over a series of temperatures; thus, the sampled potential energy range is largely expanded, to both low and high energies. In the present study, we used 100 discrete temperatures evenly spaced in the range 50−300 K. In the ITS simulation, the system is governed with a biased potential function $U'(r) = U + f(U)$, where U is the potential energy of a standard MD simulation and $f(U)$ is a function of U. An equilibrium simulation with ITS yields a distribution function

$$\rho'(r) = e^{-\beta U'(r)}/Q' \tag{1}$$

where $\beta = 1/k_B T$, with k_B being the Boltzmann constant, T being the temperature, and $Q' = \int e^{-\beta' U(r)}\,dr$. In ITS, since $U'(r)$ is a known function of $U(r)$, the distribution function $\rho(r)$ for the original system with the unbiased potential can be recovered from $\rho'(r)$ as

$$\rho(r) = \frac{e^{-\beta U(r)}}{Q} = \rho'(r) = \frac{e^{-\beta[U(r)-U'(r)]}Q'}{Q} \tag{2}$$

where $Q = \int e^{-\beta U(r)}\,dr$. More details on the method can be found in our previous publications.[2,59]

The majority of the DFT calculations were performed with the Gaussian 09 program package.[60] The BLYP-M2 calculations were performed with the GAMESS package,[61] and additional MP2 minimizations mentioned below were performed with the PQS package.[62] The structures of $(H_2O)_{12}$ and $(H_2O)_{20}$ were optimized using the BLYP-M2 approach[44] with the aug-cc-pVDZ[63] basis set. The BLYP-M2 approach was trained to best reproduce the coupled cluster quality potential energy surface for water and include both short-range and long-range corrections to the BLYP functional. DFT optimizations of $LiI(H_2O)_n$ and $CsI(H_2O)_n$ (n = 10, 18, and 20) were performed with the long-range corrected hybrid functional LC-ωPBE.[64−67] We used the standard Pople type basis 6-311++G(d,p) for Li, O, and H atoms, and the effective core potential (ECP) basis sets LANL2DZdp[68] for Cs and I atoms. For the $(H_2O)_{20}$ cluster, dispersion-corrected ωB97XD[69] and B2PLYPD[70] functionals were also utilized with the 6-311++G(d,p) basis set. The basis sets were obtained from the EMSL basis set library.[71] The combination of the LC-ωPBE functional and the above basis sets was shown to give reasonable agreement between theoretical and experimental vertical detachment energies of smaller cluster $LiI(H_2O)_n^-$ and $CsI(H_2O)_n^-$ (n = 0−6).[43] After structure optimization, harmonic vibrational frequencies were calculated to confirm the structures were indeed local minima. Zero-point vibrational energy correction was incorporated to all the energies reported unless otherwise noted. The zero-point vibrational energy

contribution to the relative cluster energy can be as large as 0.6 kcal/mol for some clusters. This contribution is significant considering the relative energy differences between some of our clusters are small.

RESULTS AND DISCUSSION

Validation of the ITS Based Minimal Energy Structure Identification Method Using $(H_2O)_{12}$ and $(H_2O)_{20}$ Clusters as Examples. To test the validity of our method, we first performed calculations on the well-studied water clusters, $(H_2O)_{12}$ and $(H_2O)_{20}$. Figure 1 shows the potential energies of the clusters in both ITS and standard MD simulations. A temperature range of 50−300 K was used in the ITS simulations (see the Computational Details). As can be seen from Figure 1, ITS allows a much broader potential energy range to be sampled when compared to standard MD simulations which were performed at 200 K for $(H_2O)_{12}$ and 170 K for $(H_2O)_{20}$. Therefore, in ITS simulations, the structure transitions over energy barriers are largely facilitated and at the same time frequent visits to low-energy structures allow the identification of many local minima.

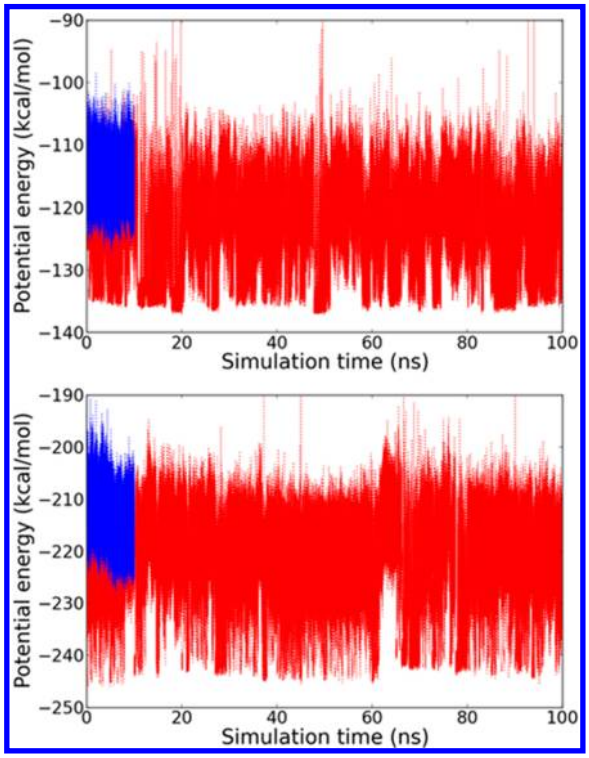

Figure 1. The evolution of the potential energy in the simulations of $(H_2O)_{12}$ (top) and $(H_2O)_{20}$ (bottom). The data shown in blue are obtained from standard MD simulations without any biased potential. The data in red are the results from the ITS simulations, in which a broad potential energy distribution is seen.

After the ITS simulations, energy minimization was first performed using the same SPC/E force field used for ITS. The optimized structures were then reoptimized with BLYP-M2. The BLYP-M2 structures are shown in Figure 2. Three of the four structures have been reported previously.[47] For the known structures, with zero-point energy correction, BLYP-M2 predicts the cage (structure B) to be more stable than the fused-cube (structure D), prism slightly above fused-cube. Without zero-point energy correction, BLYP-M2 actually predicts the fused-cube to be the more stable than the cage by 0.18 kcal/mol. A verification with MP2 at the aug-cc-pVDZ basis set shows that the fused-cube is more stable by 1.49 kcal/mol at the corresponding BLYP-M2 geometry. Thus, even with zero-point correction, MP2 is likely to predict the fused-cube to be more stable, as indicated previously with a slightly smaller basis set.[47] The newly found structure C is more stable than the fused-cube according to the SPC/E force field. However, this structure is 1.54 kcal/mol higher in energy when compared with the fused-cube structure. Each of the water molecules in the cage structure forms three hydrogen bonds with other water molecules. Structure C is similar to the cage structure, but one of the water molecules in structure C forms two hydrogen bonds. In the ITS simulation trajectory, we found that the transition between the cage and prism structures undergoes the newly identified cage-like structure C. Thus, structure C is likely to be an intermediate local minimum if a long-time real standard molecular dynamics simulation is performed (we note here that real time dynamics behavior is missed in the enhanced sampling simulations including ITS).

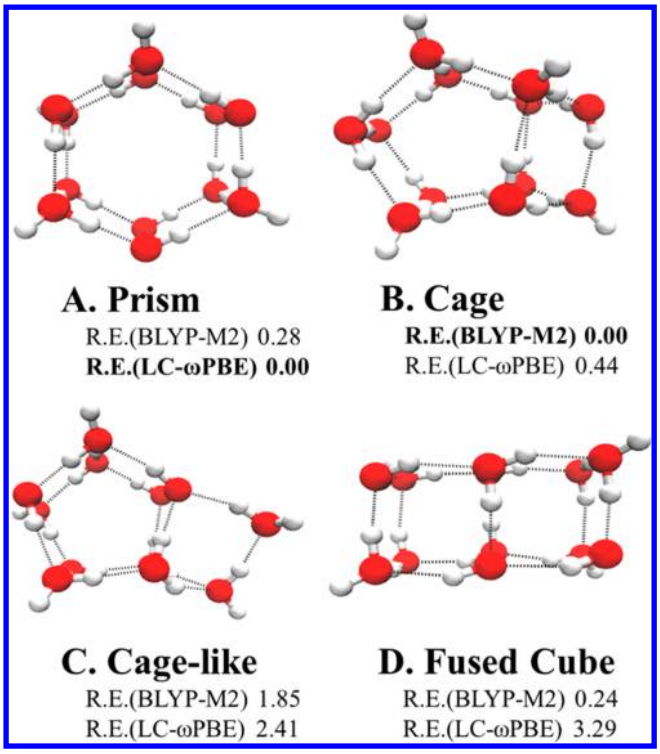

Figure 2. Stable structures and the relative energies of $(H_2O)_{12}$, with their energies given relative to the most stable one in units of kcal/mol. (The names for structures A, B, and D are taken from the study of A. Lenz et al.[47]). The BLYP-SP and MP2 single-point energy results are given in the Supporting Information in Table S2.

Figure 3 shows the BLYP-M2 structures for $(H_2O)_{20}$. The edge sharing pentagonal prism (structure C) was the putative global minimum established previously.[46−53,72−74] Including zero-point energy correction, BLYP-M2 suggests that structure A is actually more stable than structure C by 0.31 kcal/mol. Without zero-point energy correction, BLYP-M2 actually predicts structure C to be lower in energy by 0.07 kcal/mol. This energy difference is below the limit of accuracy of the BLYP-M2 approach. We performed geometry optimizations using the MP2 method with the aug-cc-pVDZ basis set and followed by MP2 energy calculations with the aug-cc-pVTZ

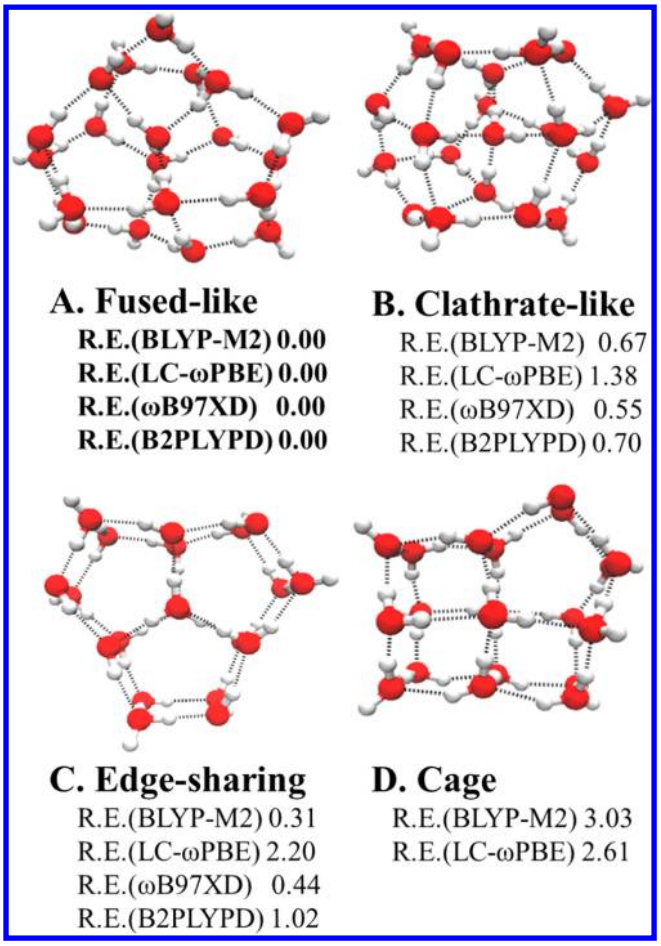

Figure 3. Stable structures and the relative energies of $(H_2O)_{20}$, with their energies given relative to the most stable structure in units of kcal/mol. The BLYP-M2 ZPE was evaluated at the BLYP-M2 geometry. The BLYP-SP and MP2 single-point energy results are given in the Supporting Information in Table S2.

basis set. MP2/aug-cc-pVTZ at the aug-cc-pVDZ geometry predicts structure C to be more stable by 0.91 kcal/mol. If zero-point vibrational energy from BLYP-M2 is incorporated to the MP2 single point energy, structure C will be more stable than structure A by 0.53 kcal/mol.

Three other functionals were also employed in the calculation. With zero-point energy correction and the 6-311++G(d,p) basis set, it was found that structure A is more stable than structure C by 2.20, 0.44, and 1.12 kcal/mol when LC-ωPBE, ωB97XD, and B2PLYPD functionals are used, respectively.

In structure B, one water molecule stays in the center of the cage formed by the other 19 water molecules. Although missing one water molecule in the cage, structure B is rather similar to the dodecahedral cage structure that is part of a clathrate hydrate; therefore, we name structure B a clathrate-like structure. Structure D was regarded as a cage structure and is similar to the previously reported one.[46] (We note here that much higher energy structures of $(H_2O)_{20}$ were also mentioned by other studies.[47−53,72−74])

Minimal Energy Structures of $LiI(H_2O)_{10}$. Following the same procedure used for the pure-water clusters, we identified low-energy structures of $LiI(H_2O)_{10}$, shown in Figure 4a. The lowest-energy structure has C_{2v} symmetry. In this structure, Li^+ and I^- are not in direct contact and each coordinates with four water molecules. Li^+ is buried inside the cluster, and I^-, on the other hand, resides on the surface. In the other low-energy structures, the coordination of both Li^+ and I^- remains essentially unchanged. These structures differ from each other by the rearrangement of hydrogen bonds between water molecules. It is interesting to note that our earlier study[43] on smaller $LiI(H_2O)_n$ clusters showed that, as long as the number of water molecules exceeds five, Li^+ and I^- become separated by water molecules. It is also worthwhile to point out that the coordination number of both ions is the same for $LiI(H_2O)_{10}$ and $LiI(H_2O)_6$, with Li^+ and I^- being coordinated with four oxygen atoms and four adjacent hydrogen atoms, respectively.

Minimal Energy Structures of $CsI(H_2O)_{10}$. The minimal energy structures of the $CsI(H_2O)_{10}$ cluster are given in Figure 4b. Cs^+ and I^- are in close contact in these low-energy structures. Both Cs^+ and I^- coordinate with three water molecules in structures A and B and with four water molecules in structures C and D, as shown in Figure 4b. These structures of $CsI(H_2O)_{10}$ are distinctly different from those of $LiI(H_2O)_{10}$ but resemble reasonably well the corresponding minima of

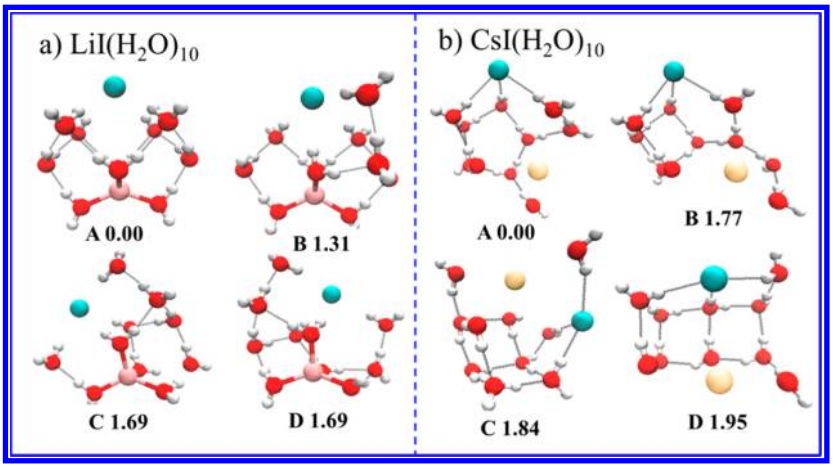

Figure 4. The most stable four structures of $LiI(H_2O)_{10}$ and $CsI(H_2O)_{10}$ and their energies relative to the most stable one. All energies are zero-point energy (ZPE) corrected and in kcal/mol. Atoms are drawn as spheres and in different colors: Li^+ in pink, Cs^+ in yellow, I^- in blue, oxygen in red, and hydrogen in gray.

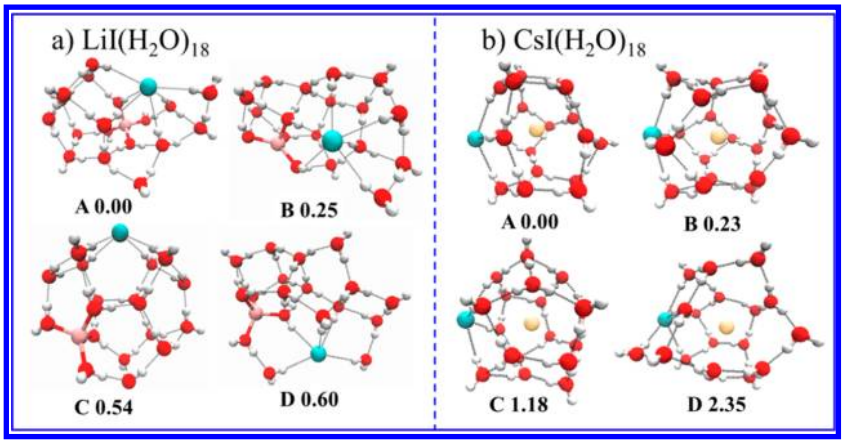

Figure 5. The four stable structures of $LiI(H_2O)_{18}$ and $CsI(H_2O)_{18}$ and their energies relative to the most stable one. All energies are zero-point energy (ZPE) corrected and in kcal/mol. Atoms are drawn as spheres and in different colors: Li^+ in pink, Cs^+ in yellow, I^- in blue, oxygen in red, and hydrogen in gray.

$(H_2O)_{12}$ clusters (see Figure 2). Structures A and D of the $CsI(H_2O)_{10}$ cluster are geometrically similar to the cage and fused-cube structures of $(H_2O)_{12}$, respectively, with two adjacent water molecules substituted by Cs^+ and I^-, respectively. In all of these low-energy structures, Cs^+ and I^- ions are in direct contact with each other, showing completely different behavior when compared to Li^+ and I^- ions.

Minimal Energy Structures of $LiI(H_2O)_{18}$ and $CsI(H_2O)_{18}$ Clusters. The core structures of $LiI(H_2O)_{18}$ and $CsI(H_2O)_{18}$ well resemble those of $LiI(H_2O)_{10}$ and $CsI(H_2O)_{10}$, respectively, showing the importance and stability of these core structures of the hydrated ions. Figure 5a shows several most stable structures of $LiI(H_2O)_{18}$ in which the $Li(H_2O)_4^+$ structural motif remains intact. I^- ion resides on the cluster surface with a coordination number of 6 in structures A and B. When the coordination number of I^- ion becomes 4 (structure C) or 5 (structure D), the energies of the system are larger than hexa-coordinated structure B by 0.29 or 0.35 kcal/mol, respectively.

I^- also resides on the surface of the $CsI(H_2O)_{18}$ cluster and coordinates with four adjacent water hydrogen atoms, as shown in Figure 5b. The Cs^+ ion is located in the center of the cage formed by 18 water molecules and the I^- in all four most stable structures. These structures of $CsI(H_2O)_{18}$ are the ones with the lowest energies and closely resemble the clathrate-like structure of $(H_2O)_{20}$ (see Figure 3). In contrast, the clathrate-like structure in $(H_2O)_{20}$ is relatively high in energy. In the clathrate-like structure of $CsI(H_2O)_{18}$ and $(H_2O)_{20}$, the central Cs^+ and water molecule coordinate with six and four molecules (for Cs^+, I^- ion is also included), respectively. Therefore, it can be concluded that the Cs^+–water interaction stabilizes the clathrate-like structure. On the other hand, the burial of a water molecule in the center of the cage of $(H_2O)_{20}$ causes an energy penalty compared to the fused and fused-like structures.

Figure 6 shows a comparison of the most stable structures of $MI(H_2O)_{10}$ and $MI(H_2O)_{18}$ (M = Li or Cs) with the structures of $(H_2O)_{12}$ and $(H_2O)_{20}$, respectively. We also calculated the $LiI(H_2O)_{20}$ and $CsI(H_2O)_{20}$ clusters following the same strategy. Their structural and energetic information is given in the Supporting Information.

Formation of Contact versus Solvent-Separated Ion Pairs. After the relative stabilities of these ion structures are known, we try to understand the number of water molecules needed for the solvent-separated ion pair (SIP) to be more stable than the contact ion pair (CIP) and similarly the double-solvent-separated ion pair (2SIP) to be more stable than SIP for a particular salt.[26] In Figure 7, we plotted the relative ion-pair distance, which is defined as the ratio of the distance between the cation and anion and the corresponding distance between such ion pairs in a vacuum; the latter is estimated by a geometry optimization in the gas phase. This figure also indicates that Li^+/I^- and Cs^+/I^- ion pairs behave very differently when hydrated. The CIP of Li^+/I^- is only found in clusters with $n \leq 4$. When $n = 5$ or 6, the two ions share one water molecule in between and are thus already in a SIP form. For all other LiI–water clusters studied, the ion pair takes the form of 2SIP. This gradual yet easy separation of the Li^+/I^- ion pair by water molecules indicates an effective dissolving of the

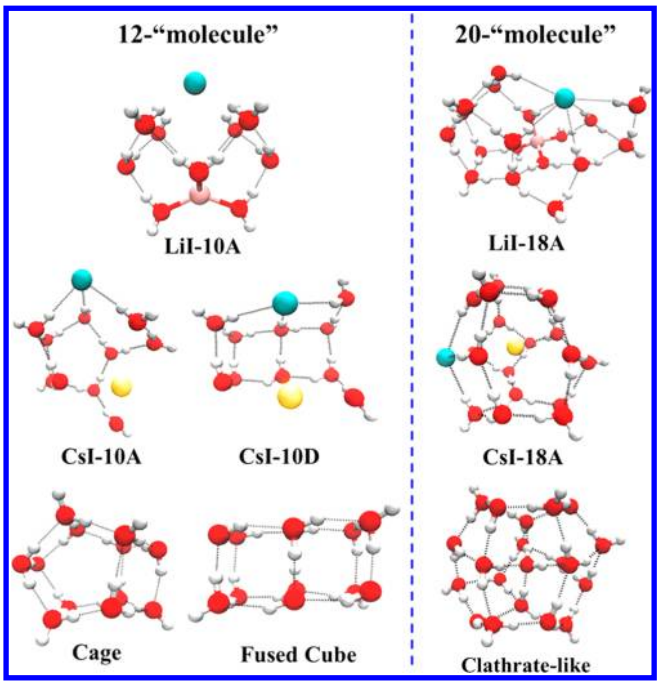

Figure 6. Comparison of the low-energy structures of $LiI(H_2O)_n$ and $CsI(H_2O)_n$ (n = 10 and 18) to the basic structures of $(H_2O)_{n+2}$ (n = 10 and 18) clusters. LiI-10A, LiI-18A, CsI-10A, and CsI-18A are the most stable ones in the corresponding clusters. Atoms are drawn in spheres and in different colors, that is, Li^+ in pink, Cs^+ in yellow, I^- in blue, oxygen in red, and hydrogen in gray.

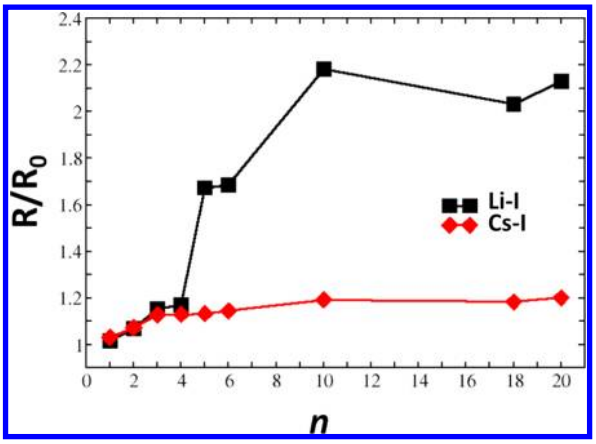

Figure 7. The ratio of average ion pair distances over the bare ion pair distance plotted as a function of the number of water molecules in the cluster. Each dot is calculated from the most stable structure of the certain number of water molecule. For the label on the *Y* axis, *R* stands for the ion pair distance in the optimized salt−water clusters with different numbers of water molecules and R_0 stands for the optimized bare ion pair distance.

two ions by a relatively small number of water molecules. On the other hand, the Cs^+/I^- ion pair remains in relatively close contact for all the clusters studied, which likely results from the weak interaction of these two ions with water.

In this paper, we only focus on the cation−anion distance evolution in neutral clusters. Nevertheless, it may be of interest to investigate the corresponding distance evolution in anionic clusters, in which the degrees of freedom that the excess electron brings in must be considered.

In addition to the stable structures, the ITS method also allows us to obtain the population of structures (calculated using the classical force field) and thus the distribution functions of cation−anion distance, as a function of temperature. These thermodynamic properties are readily calculated through a reweighting procedure.[2] Figure 8 shows that the Cs^+−I^- distance remains largely constant in the temperature range 75−275 K, in either $CsI(H_2O)_{10}$ or $CsI(H_2O)_{18}$. The Li^+−I^- distance in the $LiI(H_2O)_{10}$ cluster, on the other hand, varies more significantly, with the most probable distance being ∼4.6 Å at 75 K and ∼4.3 Å at 100 K. The Li^+−I^- distance distribution for $LiI(H_2O)_{18}$ also shows more features. At least two kinds of structures exist, with the distances of cation and anion being ∼4.6 and ∼6.0 Å, respectively. These results again indicate that it is more difficult for the Cs^+/I^- ion pair to be separated by water, whereas the Li^+/I^- ion pair exists in several different solvent-separated structures with varying Li^+−I^- distance. In the Supporting Information, we also give the structure assignment and discussions of the temperature effect on cation−anion distance distributions for $LiI(H_2O)_{10}$ and $LiI(H_2O)_{20}$ clusters.

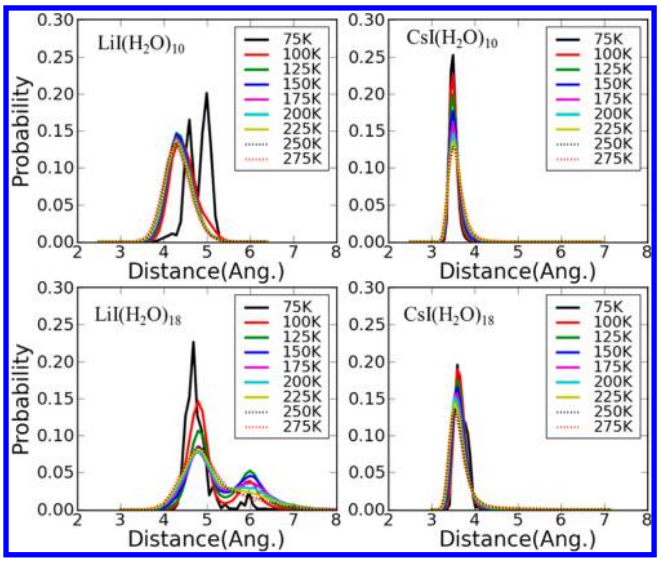

Figure 8. Cation−anion distance distribution of different clusters at a series of selected temperatures. These data are obtained from ITS simulation trajectories.

Ion Effects on Water−Water Hydrogen Bonding. One of the most debated questions is whether and how ions affect the water−water interactions.[8,10,75] In this paper, we first compare the properties of the hydrogen bonds formed by water molecules before and after the two ion pairs are added, focusing on the most stable structures of $LiI(H_2O)_{18}$, $CsI(H_2O)_{18}$, and $(H_2O)_{20}$. For simplicity, in this study, a hydrogen bond is formed if the oxygen−oxygen distance is less than 3.5 Å and the (O−H−O) angle is larger than 120°. (These criteria are slightly more strict than the definition used by Xenides et al.[76] for liquid water.) Table 1 indicates that the addition of Li^+/I^- or Cs^+/I^- changes the number of dangling hydrogen (free hydrogen) atoms slightly. The average hydrogen bond angles and lengths are also different in the two types of salt−water clusters. The Li^+ and I^- ions make an average water−water hydrogen bond shorter and the O−H−O angle larger when compared to pure-water clusters. On the contrary, the Cs^+ and I^- ions do not significantly change the O−H−O angle and only slightly shorten the hydrogen bond. Thus, LiI has a stronger capability of increasing the strength of individual water−water hydrogen bonds.

Table 1. The Number of Free Hydrogens and the Average Hydrogen Bond Angle and Length in the Most Stable Structure of $LiI(H_2O)_{18}$, $CsI(H_2O)_{18}$, and $(H_2O)_{20}$ Clusters

	free H	angle (deg)	length (Å)
$(H_2O)_{20}$	8	163.717	2.868
$LiI(H_2O)_{18}$	9	169.059	2.778
$CsI(H_2O)_{18}$	7	164.894	2.784

We also calculated the numbers of hydrogen bonds formed by each water molecule and classify each hydrogen bond as a hydrogen donor or a hydrogen acceptor bond. According to the numbers of donor (D) and acceptor (A) hydrogen bonds formed, the most populated four types, 1D1A, 1D2A, 2D1A, and 2D2A, are taken into consideration in this paper. The populations of the four types of water molecules for the most stable structures of $(H_2O)_{20}$, $LiI(H_2O)_{18}$, and $CsI(H_2O)_{18}$ clusters are given in Table 2.

It is clear from Table 2 that water molecules tend to have a higher coordination number in $CsI(H_2O)_{18}$ than in $LiI(H_2O)_{18}$. This is especially true for water bound to Cs^+. In contrast, binding with Li^+ makes the water molecules less coordinated. The same trend is observed for both the minimal energy clusters and the average number of hydrogen bonds obtained in the ITS simulations. From Figure 9, it is clear that the lower average coordination number for water in the $LiI(H_2O)_{18}$ cluster is mainly due to the existence of a larger number of

Table 2. The Populations of Different Types of Water Molecules in the Most Stable Structure of $LiI(H_2O)_{18}$, $CsI(H_2O)_{18}$, and $(H_2O)_{20}$ Clusters

	2D2A	2D1A	1D2A	1D1A
$(H_2O)_{20}$	5	7	7	1
$LiI(H_2O)_{18}$	2	7	5	4
$CsI(H_2O)_{18}$	6	5	7	0

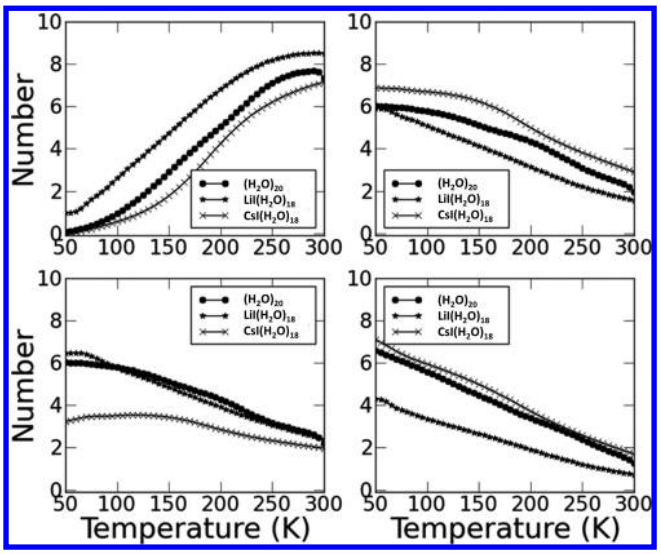

Figure 9. Averaged number of coordinated water molecules in 1D1A (upper left), 1D2A (upper right), 2D1A (bottom left), and 2D2A (bottom right) types. These data are obtained from ITS simulation trajectories of $(H_2O)_{20}$, $LiI(H_2O)_{18}$, and $CsI(H_2O)_{18}$ clusters. Here one water molecule bound to a cation (anion) is also counted as a hydrogen acceptor (donor).

1D1A. Cs^+ and I^- ions increase the populations of 1D2A and 2D2A in the temperature range 50−300 K, while Li^+ and I^- mainly increase the number of 2D1A at low temperatures. These results indicate the complicated nature of salt effects on water structure and interactions. LiI strengthens hydrogen bonds in the first solvation shell of the Li^+ but weakens the overall hydrogen bonding network by making water molecules less coordinated (see Table 2 and Figure 9).

CONCLUSION

This study shows that the ion−water cluster structures are strongly influenced by the delicate balance between ion−water and water−water interactions. $LiI(H_2O)_n$ and $CsI(H_2O)_n$ (n = 10, 18, and 20) possess very different minimal energy configurations according to DFT. Compared to the pure-water clusters containing the same number of heavy atoms, the Li^+ ion induces large structural changes. The Li^+, commonly believed to be strongly hydrated in bulk water,[77,78] interacts favorably with water and becomes fully hydrated as long as the cluster contains more than five water molecules. The structures of $LiI(H_2O)_{10}$ and $LiI(H_2O)_{18}$ (and $LiI(H_2O)_{20}$ shown in the Supporting Information) can all be viewed as being built around the $Li^+(H_2O)_4$ structural motif. For all three clusters, both Li^+ and I^- coordinate with four water molecules. Li^+ is enclosed inside the cluster, and I^- is exposed at the cluster surface. Notably, the tetra-coordinated Li^+ also possesses the dominant percent in lithium aqueous solutions according to the previous studies.[77,78] The difference in lithium coordination numbers between theory and bulk experiments cannot be adequately addressed by these cluster studies.

On the other hand, the ion−water and cation−anion interaction are weak in $CsI(H_2O)_n$ clusters, which results in the preservation of much of the overall structures of the corresponding pure-water clusters in both $CsI(H_2O)_{10}$ and $CsI(H_2O)_{18}$. For smaller clusters, Cs^+ stays at the cluster surface and when the number of available water molecules becomes large, it is buried inside the cluster. The coordination numbers of Cs^+ and I^- are both 4 when n = 10, while, for n = 18 or 20, they tend to coordinate with more water molecules (oxygen or hydrogen atoms). The structural features of $(H_2O)_{12}$ (cage and face-sharing fused-cube) remain largely unchanged in $CsI(H_2O)_{10}$. In the latter, the two ions occupy the positions of two water molecules of the $(H_2O)_{12}$, and I^- is partially exposed. The clathrate-like structure, which is relatively unstable for $(H_2O)_{20}$, becomes the lowest-energy structure in $CsI(H_2O)_{18}$, largely due to the Cs^+'s coordination with six water molecules which makes its residence in the center of the cage much favored. As a result of the dominant water−water interaction, the change of two water molecules to one Cs^+ and one I^- does not alter significantly the overall structures of $(H_2O)_{12}$ or $(H_2O)_{20}$, although it does change the relative stability of the structures (see Figures 3 and 5). In summary, the electrostatic interaction is weaker between the Cs^+/I^- ion pair, but their interactions with water molecules are also weaker. By forming an ion pair, the clusters permit better water−water interactions. Such an argument is consistent with the "matching water affinity" argument used in understanding ion pairing in bulk solutions.

The different properties of the two types of salt−water clusters also show in the cation−anion distances. Li^+−I^- forms a stable SIP when the number of water molecules reaches 5, while Cs^+−I^- remains as a CIP form. For $n \geq 10$, Li^+−I^- prefers 2SIP but Cs^+−I^- still remains in close contact. It is expected that more water molecules would insert to the ion pairs and make the ion pairs more apart both in $LiI(H_2O)_n$ and $CsI(H_2O)_n$ clusters as the cluster size further increases, but the number of water molecules needed is larger than that used in the current study.

ASSOCIATED CONTENT

Supporting Information

The MM and QM energy correlation diagrams and structures, discussions on the temperature effect, the BLYP-SP and MP2 single-point energy results, and the coordinates and energetics information. This material is available free of charge via the Internet at http://pubs.acs.org.

AUTHOR INFORMATION

Corresponding Authors

*E-mail: zhengwj@iccas.ac.cn.
*E-mail: gaoyq@pku.edu.cn.

Notes

The authors declare no competing financial interest.

ACKNOWLEDGMENTS

Y.Q.G. acknowledges National Key Basic Research Foundation of China (2012CB917304) and NSFC (91027044, 21233002, and 21125311) for support. W.-J.Z. acknowledges the Institute of Chemistry, Chinese Academy of Sciences, for start-up funds. F.W. acknowledges Dr. Peter Pulay for helpful discussions.

REFERENCES

(1) Gao, Y. Q. An Integrate-over-Temperature Approach for Enhanced Sampling. *J. Chem. Phys.* **2008**, *128*, 064105−064109.

(2) Gao, Y. Q. Self-Adaptive Enhanced Sampling in the Energy and Trajectory Spaces: Accelerated Thermodynamics and Kinetic Calculations. *J. Chem. Phys.* **2008**, *128*, 134111−134118.

(3) Cserháti, T.; Forgács, E. Effect of Ph and Sodium Chloride on the Strength and Selectivity of the Interaction of [Tau]-Cyclodextrin with Some Antisense Nucleosides. *Int. J. Pharm.* **2003**, *254*, 189−196.

(4) Asmar, B. N.; Ergenzinger, P. Long-Term Prediction of the Water Level and Salinity in the Dead Sea. *Hydrol. Processes* **2002**, *16*, 2819−2831.

(5) Oum, K. W.; Lakin, M. J.; DeHaan, D. O.; Brauers, T.; Finlayson-Pitts, B. J. Formation of Molecular Chlorine from the Photolysis of Ozone and Aqueous Sea-Salt Particles. *Science* **1998**, *279*, 74−77.

(6) Knipping, E. M.; Lakin, M. J.; Foster, K. L.; Jungwirth, P.; Tobias, D. J.; Gerber, R. B.; Dabdub, D.; Finlayson-Pitts, B. J. Experiments and Simulations of Ion-Enhanced Interfacial Chemistry on Aqueous Nacl Aerosols. *Science* **2000**, *288*, 301−306.

(7) Finlayson-Pitts, B. J. The Tropospheric Chemistry of Sea Salt: A Molecular-Level View of the Chemistry of Nacl and Nabr. *Chem. Rev.* **2003**, *103*, 4801−4822.

(8) Gao, Y. Q. Simple Theoretical Model for Ion Cooperativity in Aqueous Solutions of Simple Inorganic Salts and Its Effect on Water Surface Tension. *J. Phys. Chem. B* **2011**, *115*, 12466−12472.

(9) Gao, Y. Q. Simple Theory for Salt Effects on the Solubility of Amide. *J. Phys. Chem. B* **2012**, *116*, 9934−9943.

(10) Yang, L. J.; Fan, Y. B.; Gao, Y. Q. Differences of Cations and Anions: Their Hydration, Surface Adsorption, and Impact on Water Dynamics. *J. Phys. Chem. B* **2011**, *115*, 12456−12465.

(11) Collins, K. D.; Neilson, G. W.; Enderby, J. E. Ions in Water: Characterizing the Forces That Control Chemical Processes and Biological Structure. *Biophys. Chem.* **2007**, *128*, 95−104.

(12) Flores, S. C.; Kherb, J.; Konelick, N.; Chen, X.; Cremer, P. S. The Effects of Hofmeister Cations at Negatively Charged Hydrophilic Surfaces. *J. Phys. Chem. C* **2012**, *116*, 5730−5734.

(13) Kunz, W.; Henle, J.; Ninham, B. W. 'Zur Lehre Von Der Wirkung Der Salze' (About the Science of the Effect of Salts): Franz Hofmeister's Historical Papers. *Curr. Opin. Colloid Interface Sci.* **2004**, *9*, 19−37.

(14) Ault, B. S. Infrared Spectra of Argon Matrix-Isolated Alkali Halide Salt/Water Complexes. *J. Am. Chem. Soc.* **1978**, *100*, 2426−2433.

(15) Gregoire, G.; Mons, M.; Dedonder-Lardeux, C.; Jouvet, C. Is Nai Soluble in Water Clusters? *Eur. Phys. J. D* **1998**, *1*, 5−7.

(16) Gregoire, G.; Mons, M.; Dimicoli, I.; Dedonder-Lardeux, C.; Jouvet, C.; Martrenchard, S.; Solgadi, D. Femtosecond Pump-Probe Ionization of Small Nai-S-N Clusters, S: H2o,Nh3: A Tool to Probe the Structure of the Cluster. *J. Chem. Phys.* **2000**, *112*, 8794−8805.

(17) Dedonder-Lardeux, C.; Gregoire, G.; Jouvet, C.; Martrenchard, S.; Solgadi, D. Charge Separation in Molecular Clusters: Dissolution of a Salt in a Salt-(Solvent)n Cluster. *Chem. Rev.* **2000**, *100*, 4023−4037.

(18) Max, J. J.; Chapados, C. Ir Spectroscopy of Aqueous Alkali Halide Solutions: Pure Salt-Solvated Water Spectra and Hydration Numbers. *J. Chem. Phys.* **2001**, *115*, 2664−2675.

(19) Zhang, Q.; Carpenter, C. J.; Kemper, P. R.; Bowers, M. T. On the Dissolution Processes of Na2l+ and Na3l2+ with the Association of Water Molecules: Mechanistic and Energetic Details. *J. Am. Chem. Soc.* **2003**, *125*, 3341−3352.

(20) Mizoguchi, A.; Ohshima, Y.; Endo, Y. Microscopic Hydration of the Sodium Chloride Ion Pair. *J. Am. Chem. Soc.* **2003**, *125*, 1716−1717.

(21) Blades, A. T.; Peschke, M.; Verkerk, U. H.; Kebarle, P. Hydration Energies in the Gas Phase of Select (MX)(M)M+ Ions, Where M+ = Na+, K+, Rb+, Cs+, Nh4(+) and X- = F-, Cl-, Br-, I-, NO2-, NO3- . Observed Magic Numbers of (MX)(M)M+ Ions and Their Possible Significance. *J. Am. Chem. Soc.* **2004**, *126*, 11995−12003.

(22) Woon, D. E.; Dunning, T. H. The Pronounced Effect of Microsolvation on Diatomic Alkali-Halides- Ab-Initio Modeling of Mx(H2O)n (M=Li, Na, X=F, Cl, N=1−3). *J. Am. Chem. Soc.* **1995**, *117*, 1090−1097.

(23) Peslherbe, G. H.; Ladanyi, B. M.; Hynes, J. T. Trajectory Study of Photodissociation Dynamics in the Nai(H2o) Cluster System. *J. Phys. Chem. A* **1998**, *102*, 4100−4110.

(24) Petersen, C. P.; Gordon, M. S. Solvation of Sodium Chloride: An Effective Fragment Study of Nacl(H2O)n. *J. Phys. Chem. A* **1999**, *103*, 4162−4166.

(25) Peslherbe, G. H.; Ladanyi, B. M.; Hynes, J. T. Free Energetics of NaI Contact and Solvent-Separated Ion Pairs in Water Clusters. *J. Phys. Chem. A* **2000**, *104*, 4533−4548.

(26) Jungwirth, P. How Many Waters Are Necessary to Dissolve a Rock Salt Molecule? *J. Phys. Chem. A* **2000**, *104*, 145−148.

(27) Yamabe, S.; Kouno, H.; Matsumura, K. A Mechanism of the Ion Separation of the NaCl Microcrystal Via the Association of Water Clusters. *J. Phys. Chem. B* **2000**, *104*, 10242−10252.

(28) Jungwirth, P.; Tobias, D. J. Molecular Structure of Salt Solutions: A New View of the Interface with Implications for Heterogeneous Atmospheric Chemistry. *J. Phys. Chem. B* **2001**, *105*, 10468−10472.

(29) Godinho, S.; do Couto, P. C.; Cabral, B. J. C. Photochemistry of AgCl-Water Clusters: Comparison with Cl–Water Clusters. *Chem. Phys. Lett.* **2006**, *419*, 340−345.

(30) Olleta, A. C.; Lee, H. M.; Kim, K. S. Ab Initio Study of Hydrated Sodium Halides NaX(H2O) 1–6 (X = F, Cl, Br, and I). *J. Chem. Phys.* **2006**, *124*, 024321−024313.

(31) Olleta, A. C.; Lee, H. M.; Kim, K. S. Ab Initio Study of Hydrated Potassium Halides KX(H2O)(1−6) (X=F,Cl,Br,I). *J. Chem. Phys.* **2007**, *126*, 144311−144321.

(32) Sciaini, G.; Fernandez-Prini, R.; Estrin, D. A.; Marceca, E. Short-Range and Long-Range Solvent Effects on Charge-Transfer-to-Solvent Transitions of I- and K+I- Contact Ion Pair Dissolved in Supercritical Ammonia. *J. Chem. Phys.* **2007**, *126*, 174504−174511.

(33) Pettitt, B. M.; Rossky, P. J. Alkali Halides in Water: Ion–Solvent Correlations and Ion–Ion Potentials of Mean Force at Infinite Dilution. *J. Chem. Phys.* **1986**, *84*, 5836−5844.

(34) Belch, A. C.; Berkowitz, M.; McCammon, J. A. Solvation Structure of a Sodium Chloride Ion Pair in Water. *J. Am. Chem. Soc.* **1986**, *108*, 1755−1761.

(35) Smith, D. E.; Dang, L. X. Computer Simulations of Nacl Association in Polarizable Water. *J. Chem. Phys.* **1994**, *100*, 3757−3766.

(36) Asada, T.; Nishimoto, K. Monte Carlo Simulations of M+Cl−(H2O)n (M = Li, Na) Clusters and the Dissolving Mechanism of Ion Pairs in Water. *Chem. Phys. Lett.* **1995**, *232*, 518−523.

(37) Asada, T.; Nishimoto, K. Monte Carlo Simulation of M+Cl−(H2O)n (M = Li, Na) Clusters−Structures, Fluctuations and Possible Dissolving Mechanism. *Mol. Simul.* **1996**, *16*, 307−319.

(38) Siu, C.-K.; Fox-Beyer, B. S.; Beyer, M. K.; Bondybey, V. E. Ab Initio Molecular Dynamics Studies of Ionic Dissolution and Precipitation of Sodium Chloride and Silver Chloride in Water Clusters, NaCl(H2O)n and AgCl(H2O)n, n = 6, 10, and 14. *Chem.—Eur. J.* **2006**, *12*, 6382−6392.

(39) Krekeler, C.; Hess, B.; Site, L. D. Density Functional Study of Ion Hydration for the Alkali Metal Ions (Li+,Na+,K+) and the Halide Ions (F-,Br-,Cl-). *J. Chem. Phys.* **2006**, *125*, 054305−054311.

(40) Koch, D. M.; Timerghazin, Q. K.; Peslherbe, G. H.; Ladanyi, B. M.; Hynes, J. T. Nonadiabatic Trajectory Studies of Nai(H2O)n Photodissociation Dynamics. *J. Phys. Chem. A* **2006**, *110*, 1438−1454.

(41) Koch, D. M.; Peslherbe, G. H. Importance of Polarization in Quantum Mechanics/Molecular Mechanics Descriptions of Electronic Excited States: Nai (H2O)n Photodissociation Dynamics as a Case Study. *J. Phys. Chem. B* **2008**, *112*, 636−649.

(42) Peslherbe, G. H.; Ladanyi, B. M.; Hynes, J. T. Structure of Nai Ion Pairs in Water Clusters. *Chem. Phys.* **2000**, *258*, 201−224.

(43) Li, R. Z.; Liu, C. W.; Gao, Y. Q.; Jiang, H.; Xu, H. G.; Zheng, W. J. Microsolvation of LiI and CsI in Water: Anion Photoelectron

Spectroscopy and Ab Initio Calculations. *J. Am. Chem. Soc.* **2013**, *135*, 5190−5199.
(44) Song, Y.; Akin-Ojo, O.; Wang, F. Correcting for Dispersion Interaction and Beyond in Density Functional Theory through Force Matching. *J. Chem. Phys.* **2010**, *133*, 174115−174124.
(45) Lenz, A.; Ojamae, L. A Theoretical Study of Water Equilibria: The Cluster Distribution Versus Temperature and Pressure for (H2O)n, n=1−60, and Ice. *J. Chem. Phys.* **2009**, *131*, 134302−134314.
(46) Kazimirski, J. K.; Buch, V. Search for Low Energy Structures of Water Clusters (H2O)n, n = 20−22, 48, 123, and 293. *J. Phys. Chem. A* **2003**, *107*, 9762−9775.
(47) Lenz, A.; Ojamäe, L. On the Stability of Dense Versus Cage-Shaped Water Clusters: Quantum-Chemical Investigations of Zero-Point Energies, Free Energies, Basis-Set Effects and Ir Spectra of (H2O)12 and (H2O)20. *Chem. Phys. Lett.* **2006**, *418*, 361−367.
(48) Bravo-Perez, G.; Saint-Martin, H. A Theoretical Study of the Confinement of Methane in Water Clusters. *Int. J. Quantum Chem.* **2012**, *112*, 3655−3660.
(49) Furtado, J. P.; Rahalkar, A. P.; Shanker, S.; Bandyopadhyay, P.; Gadre, S. R. Facilitating Minima Search for Large Water Clusters at the MP2 Level Via Molecular Tailoring. *J. Phys. Chem. Lett.* **2012**, *3*, 2253−2258.
(50) Maheshwary, S.; Patel, N.; Sathyamurthy, N.; Kulkarni, A. D.; Gadre, S. R. Structure and Stability of Water Clusters (H2O)(N), N=8−20: An Ab Initio Investigation. *J. Phys. Chem. A* **2001**, *105*, 10525−10537.
(51) Tokmachev, A. M.; Tchougreeff, A. L.; Dronskowski, R. Hydrogen-Bond Networks in Water Clusters (H2O)(20): An Exhaustive Quantum-Chemical Analysis. *ChemPhysChem* **2010**, *11*, 384−388.
(52) Wales, D. J.; Hodges, M. P. Global Minima of Water Clusters (H2O)n, $n \leq 21$, Described by an Empirical Potential. *Chem. Phys. Lett.* **1998**, *286*, 65−72.
(53) Yang, F.; Wang, X.; Yang, M. L.; Krishtal, A.; van Alsenoy, C.; Delarue, P.; Senet, P. Effect of Hydrogen Bonds on Polarizability of a Water Molecule in (H2O)n (n=6, 10, 20) Isomers. *Phys. Chem. Chem. Phys.* **2010**, *12*, 9239−9248.
(54) Case, D. A.; et al. *Amber 9*; University of California, San Francisco, 2006.
(55) Berendsen, H. J. C.; Grigera, J. R.; Straatsma, T. P. The Missing Term in Effective Pair Potentials. *J. Chem. Phys.* **1987**, *91*, 6269−6271.
(56) Joung, I. S.; Cheatham, T. E. Determination of Alkali and Halide Monovalent Ion Parameters for Use in Explicitly Solvated Biomolecular Simulations. *J. Phys. Chem. B* **2008**, *112*, 9020−9041.
(57) Wu, X. W.; Brooks, B. R. Self-Guided Langevin Dynamics Simulation Method. *Chem. Phys. Lett.* **2003**, *381*, 512−518.
(58) Humphrey, W.; Dalke, A.; Schulten, K. Vmd: Visual Molecular Dynamics. *J. Mol. Graphics* **1996**, *14*, 33−38.
(59) Yang, L.; Shao, Q.; Gao, Y. Q. Thermodynamics and Folding Pathways of Trpzip2: An Accelerated Molecular Dynamics Simulation Study. *J. Phys. Chem. B* **2008**, *113*, 803−808.
(60) Frisch, M. J.; et al. *Gaussian 09*; Gaussian, Inc.: Wallingford, CT, 2009.
(61) Gordon, M. S.; Schmidt, M. W. Advances in Electronic Structure Theory: Gamess a Decade Later. *Theory Appl. Comput. Chem.: First Forty Years* **2005**, 1167−1189.
(62) Baker, J.; Wolinski, K.; Malagoli, M.; Kinghorn, D.; Wolinski, P.; Magyarfalvi, G.; Saebo, S.; Janowski, T.; Pulay, P. Quantum Chemistry in Parallel with Pqs. *J. Comput. Chem.* **2008**, *30*, 317−335.
(63) Dunning, T. H. Gaussian Basis Sets for Use in Correlated Molecular Calculations. I. The Atoms Boron through Neon and Hydrogen. *J. Chem. Phys.* **1989**, *90*, 1007−1023.
(64) Tawada, Y.; Tsuneda, T.; Yanagisawa, S.; Yanai, T.; Hirao, K. A Long-Range-Corrected Time-Dependent Density Functional Theory. *J. Chem. Phys.* **2004**, *120*, 8425−8433.
(65) Vydrov, O. A.; Scuseria, G. E. Assessment of a Long-Range Corrected Hybrid Functional. *J. Chem. Phys.* **2006**, *125*, 234109−234117.
(66) Vydrov, O. A.; Heyd, J.; Krukau, A. V.; Scuseria, G. E. Importance of Short-Range Versus Long-Range Hartree-Fock Exchange for the Performance of Hybrid Density Functionals. *J. Chem. Phys.* **2006**, *125*, 074106−074114.
(67) Vydrov, O. A.; Scuseria, G. E.; Perdew, J. P. Tests of Functionals for Systems with Fractional Electron Number. *J. Chem. Phys.* **2007**, *126*, 154109−154117.
(68) Wadt, W. R.; Hay, P. J. Ab Initio Effective Core Potentials for Molecular Calculations. Potentials for Main Group Elements Na to Bi. *J. Chem. Phys.* **1985**, *82*, 284−298.
(69) Chai, J.; Head-Gordon, M. Long-Range Corrected Hybrid Density Functionals with Damped Atom-Atom Dispersion Corrections. *Phys. Chem. Chem. Phys.* **2008**, *10*, 6615−6620.
(70) Schwabe, T.; Grimme, S. Double-Hybrid Density Functionals with Long-Range Dispersion Corrections: Higher Accuracy and Extended Applicability. *Phys. Chem. Chem. Phys.* **2007**, *9*, 3397−3406.
(71) Schuchardt, K. L.; Didier, B. T.; Elsethagen, T.; Sun, L.; Gurumoorthi, V.; Chase, J.; Li, J.; Windus, T. L. Basis Set Exchange: A Community Database for Computational Sciences. *J. Chem. Inf. Model.* **2007**, *47*, 1045−1052.
(72) Fanourgakis, G. S.; Apra, E.; Xantheas, S. S. High-Level Ab Initio Calculations for the Four Low-Lying Families of Minima of (HO). I. Estimates of MP2/CBS Binding Energies and Comparison with Empirical Potentials. *J. Chem. Phys.* **2004**, *121*, 2655.
(73) Fanourgakis, G. S.; Aprà, E.; De Jong, W. A.; Xantheas, S. S. High-Level Ab Initio Calculations for the Four Low-Lying Families of Minima of (HO). II. Spectroscopic Signatures of the Dodecahedron, Fused Cubes, Face-Sharing Pentagonal Prisms, and Edge-Sharing Pentagonal Prisms Hydrogen Bonding Networks. *J. Chem. Phys.* **2005**, *122*, 134304.
(74) Lagutschenkov, A.; Fanourgakis, G. S.; Niedner-Schatteburg, G.; Xantheas, S. S. The Spectroscopic Signature of the "All-Surface" to "Internally Solvated" Structural Transition in Water Clusters in the n= 17−21 Size Regime. *J. Chem. Phys.* **2005**, *122*, 194310.
(75) Mancinelli, R.; Botti, A.; Bruni, F.; Ricci, M. A.; Soper, A. K. Hydration of Sodium, Potassium, and Chloride Ions in Solution and the Concept of Structure Maker/Breaker. *J. Phys. Chem. B* **2007**, *111*, 13570−13577.
(76) Xenides, D.; Randolf, B. R.; Rode, B. M. Hydrogen Bonding in Liquid Water: An Ab Initio QM/MM MD Study. *J. Mol. Liq.* **2006**, *123*, 61−67.
(77) Loeffler, H. H.; Rode, B. M. The Hydration Structure of the Lithium Ion. *J. Chem. Phys.* **2002**, *117*, 110−117.
(78) Varma, S.; Rempe, S. B. Coordination Numbers of Alkali Metal Ions in Aqueous Solutions. *Biophys. Chem.* **2006**, *124*, 192−199.